Desalination and Water Treatment
www.deswater.com
doi: 10.1080/19443994.2013.855680

52 (2014) 3564–3571
May

Adsorption of Congo red from aqueous solution onto pyrolusite reductive leaching residue

Wu Shen, Bing Liao, Weiyi Sun, Shijun Su, Sanglan Ding*

Department of Environmental Science and Engineering, Sichuan University, Chengdu 610065, China
Tel. +86-28-8546 0916; *email*: dslscu@163.com

Received 27 August 2013; Accepted 20 September 2013

ABSTRACT

This study investigated the potential use of pyrolusite reductive leaching residue (PLR), a low-cost residual solid by-product in manganese hydrometallurgy, as alternative adsorbent for removal of Congo red (CR) from aqueous solution. The surface characteristics of the PLR were measured. The effect of contact time was experimentally studied to evaluate the adsorption capacity, kinetics, and equilibrium. Experimental results revealed that the adsorption process almost finished within 300 min; adsorption capacity of the PLR increased with increasing initial CR concentrations and temperature. CR uptake process obeyed the pseudo-second-order kinetics. The CR uptake process was best described by the Langmuir isotherm with maximum monolayer adsorption capacity of 45.66 mg/g at 25°C. Thermodynamic studies showed CR adsorption onto the PLR was endothermic and spontaneous in nature. The regeneration studies showed that the PLR has good reuse performance. The results indicated that PLR could be employed as low-cost alternatives for removal of CR from industrial wastewater.

Keywords: Congo red; Pyrolusite reductive leaching residue; Adsorption; Desorption; Reuse

1. Introduction

Colored wastewater, which is widely present in the effluents of textiles, rubber, paper, plastic, and cosmetics industries, may pose a severe threat to public health and the environment because of its marked carcinogenic and mutagenic effects to human and other living organisms [1,2]. Thus, there is a great need to devise available technologies to remove hazardous dyes from their aqueous solutions. A variety of techniques, such as ion exchange [3–6], chemical oxidation [7–10], biodegradation [11,12], and adsorption [13–37] have been developed for this purpose. Among these methods, adsorption is a promising technique and widely used because of its high efficiency and simple operation. But the use of activated carbon, which is the most widely used adsorbent, is not suitable for developing countries because of its high cost. The use of low-cost adsorbents such as clay minerals [13–16], industrial wastes [17–23], and agricultural wastes [24–37] were more suitable.

Manganese oxide ore is one of the most important manganese minerals, which has very high potential as a source of manganese, as well as other associated metals such as copper, nickel, and cobalt. As the ores possess a high surface area, they can also act as an effective adsorbent for removal of phosphate, selenite, phenolic compounds, and heavy metal ions from synthetic solutions and industrial wastewater [38–46]. However, it must be noted that in the manganese

---

*Corresponding author.

oxide ores used as adsorbents, only the ores are leached out of associated metals and the manganese remained unleached. These leaching residuals have the manganese content at 17–18%, which are still important sources of manganese recovery.

In recent years, manganese demand has been driven by soaring steel production. The world rapidly growing demand for manganese has made it increasingly important to develop processes for economical recovery of manganese from low grade manganese ores [47]. Various direct reductive leaching processes have been studied and developed for processing low manganese ores, including leaching with ferrous iron [48,49], organic reductants [50,51], bio-reductions [52,53], and sulfur dioxide [54–58]. Among these processes, the leaching with sulfur dioxide is proved promising attributing to the advantages of fast leaching rate, high Mn extraction rate and selectivity leaching of Mn. Moreover, electrolytic manganese production with low-grade pyrolusite leaching by SO_2 has proved to be feasible [58]. For the reasons above, from the perspective of manganese metallurgy, it is more suitable to recover manganese from these manganese ores than used as adsorbents directly. Unavoidably, once the Mn is extracted, the new waste may be produced. Compared with Mn ore, this leach residual has a low content of Mn, and the structure and surface properties may have been changed in the leaching process. Literature on this waste is scarcely seen; whether it is still used as adsorbent remained poorly understood.

In this research, the pyrolusite reductive leaching residue (PLR) was developed. Congo red (CR) (sodium salt of benzidinediazobis-1-naphthylamine-4-sulfonic acid) was selected in this study as a model anionic dye. CR has complex chemical structure and high solubility as well as is persistent in aqueous solution [59,60]. It is investigated as a mutagen and reproductive effector. It irritates skin, eye, and gastrointestinal and may affect blood factors such as clotting, as well as induce somnolence and respiratory problems [61]. Adsorption behavior of PLR toward CR was evaluated by investigating the effect of experimental parameters such as adsorbent dose and contact time, as well as studying the adsorption kinetics and isotherms. The results of this study will have important implications for adsorption technologies used to treat CR pollutants.

2. Experimental

2.1. Materials

CR, supplied by Miura chemical plant in Shanghai, was used directly without further purification. Other agents used were all analytical grade and all solutions were prepared with distilled water.

2.2. Preparation and surface characteristics of adsorbent PLR

The leaching of pyrolusite with sulfur dioxide was taken in a bubbling reactor (ID, 18.5 cm; height, 38 cm; internal volume, 10 L) under semi-batch condition (agitation speed, 300 rpm/min, temperature, 50°C). The pyrolusite slurry was prepared by mixing 5 L tap water with 2.5 Kg commercial pyrolusite first and then 6% SO_2 (1.5 m^3/h) was injected until a molar ratio of $SO_2/MnO_2 = 1.5$ was reached. Leaching residue was separated by centrifugation and washed with deionized water until the soluble salts were completely removed. The solid was oven-dried at 110°C for 24 h, and sieved to 140–200 mesh by standard sieves (Model 200). The product was referred to as PLR.

Surface area and porosities of PLR were measured by nitrogen adsorption and desorption analysis (Micrometritics, Tristar II 3020). Particle-size distribution was measured by a particle size analyzer (Malvern Instruments Corporate, Hydro 2000MU (A)). The pH at the point of zero charge (pHpzc) was estimated from a batch equilibrium method described by Babic [62]. The compositions and some physical properties of PLR are showed in Tables 1 and 2, respectively.

2.3. Adsorption experiments

Batch equilibrium CR adsorption studies were performed by mixing a known dose of PLR (0.04–0.64 g) with 50 mL solutions of certain CR concentration in a 250 mL Erlenmeyer flask, and the flasks were shaken at 200 rpm in a water bath shaker (SHA-CA) at 25 ± 1°C for 120 min to reach equilibrium. Then, the mixture was filtered and the residual CR concentrations were measured using an UV-visible spectrophotometer (UV-754, Shanghai) at a wavelength of 500 nm.

Table 1
Chemical compositions of PLR (%)

SiO_2	Fe_2O_3	Al_2O_3	CaO	SO_3	MnO_2
43.2	22.2	15.7	6.2	4.5	2.5

Table 2
Physical properties of PLR

Average particle size (μm)	Bulk density (g/cm^3)	Specific surface area (m^2/g)	Specific gravity (cm^3/g)	pH_{ZPC}
12.02	0.68	73.32	0.13	6.60

Adsorption kinetic experiments were done to investigate the effect of contact time and evaluate the kinetic properties. PLR (2.4 g) was added into 1000 ml of CR solution with initial concentrations of 100.0 mg/L. The mixture was agitated on an electromagnetic stirrer (Model 78-1) at 300 rpm and 25 ± 1℃. The stirring rate of 300 rpm was chosen to disperse PLR homogenously in solution. At preset time intervals (0–360 min), 10 mL of samples were drawn and filtered, and the residual CR concentration was analyzed by the same method described above.

2.4. Desorption experiments

For the desorption study, 0.12 g PLR were added to 50 mL of CR solutions (100 mg/L, pH 6.25), once equilibrium reached, the CR-adsorbed PLR adsorbents were separated from solution by filtration, and then stirred for 1 h in 50 mL of distilled water at different pHs. After filtration, the desorbed dye was determined to calculate the desorption efficiency.

For reuse, solutions with different NaOH concentrations were used as eluents, the same operation of adsorption–desorption mentioned above was applied first, and then the desorbed PLR adsorbents were separated and washed by distilled water. Both the desorbed PLR and desorbed NaOH solutions were used as adsorbent and eluent in subsequent cycles. The adsorption–desorption-washing was repeated over five consecutive cycles.

3. Results and discussion

3.1. Adsorption of CR onto PLR

3.1.1. Effect of contact time

Fig. 1 shows the time profile of CR removal with 2.4 g/L of PLR at different initial CR concentrations and temperatures. From Fig. 1, three important conclusions could be drawn. First, in all the concentrations the adsorption process was almost finished within 300 min, and no significant change was observed from 300 to 600 min. Second, the total amount of CR adsorbed increased with the increasing initial CR concentrations. This is because more CR is available at higher initial concentrations of CR, and higher initial adsorbate concentration provides higher driving force for the ions from the solution to the PLRs, resulting in more collisions between CR ions and active sites on the PLRs. Third, the adsorption capacity of the PLR increased with increasing of the temperature from 25 to 45℃; the higher temperature is to the advantage of adsorption and that the adsorption is an endothermic reaction.

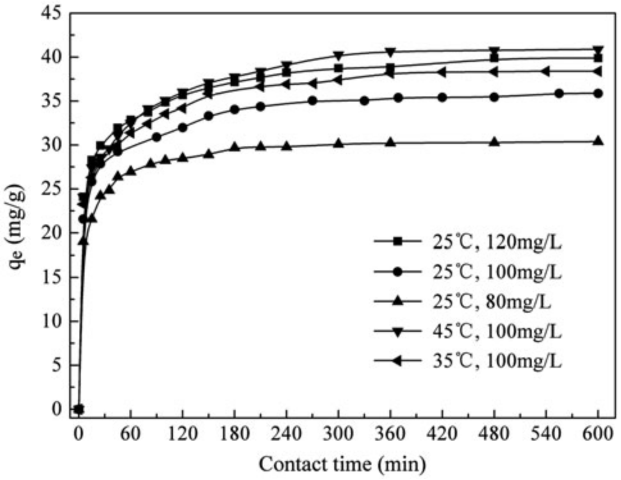

Fig. 1. Effect of contact time on CR adsorption onto PLR.

3.1.2. Adsorption kinetics

Kinetics models are used to reflect a relationship between the adsorption rate and equilibrium time. Adsorption kinetics data were analyzed by the two most widely used kinetic models, i.e. the pseudo-first-order [63] and pseudo-second-order [64] model. The non-linear forms of the two models can be expressed as:

$$q_t = q_e(1 - e^{-k_1 t}) \tag{1}$$

$$q_t = \frac{q_e^2 k_2 t}{1 + q_e k_2 t} \tag{2}$$

where q_t is the amount of dye adsorbed per unit of adsorbent (mg/g) at time t, k_1 is the pseudo-first-order rate constant (min^{-1}), and t is the treatment time (min). The adsorption rate constant (k_1) was calculated from the plot of log ($q_e - q_t$) against t. k_2 is the pseudo-second-order rate constant (gmg^{-1} min^{-1}). The q_e and k_2 can be obtained by linear plot of t/q_t vs. t.

The comparison of different kinetic models for the adsorption of CR onto PLR at different initial concentrations was conducted; all kinetic parameters and correlation coefficients are listed in Table 3. It can be seen that the calculated adsorption capacity $q_{e\ (cal.)}$ for pseudo-second-order model was much more closer to the experimental adsorption capacity $q_{e\ (exp.)}$ for various CR concentrations confirming better applicability of pseudo-second- order model compared to pseudo-first-order model. These results are further confirmed by higher regression coefficient (R_2^2) values for pseudo-second-order model compared to pseudo-first-order

Table 3
Pseudo-first and pseudo–second order adsorption kinetic parameters for the adsorption of CR onto PLR

		Lagergren-first-order			Pseudo-second-order		
C_0 (mg/L)	$q_{e(exp)}$ (mg/g)	$q_{e(cal)}$ (mg/g)	k_1 (1/min)	R_1^2	$q_{e(cal)}$ (mg/g)	k_2 (g mg^{-1} min^{-1})	R_2^2
80	30.39	6.85	0.0228	0.9467	30.77	0.0044	0.9999
100	35.87	9.44	0.0173	0.9522	36.36	0.0023	0.9997
120	39.88	11.71	0.0175	0.9662	40.49	0.0020	0.9994

model (Table 3). Additionally, higher surface loadings would result in lower diffusion efficiency and a high competition of anionic dye for fixed reaction sites, consequently, the value of rate constant k_2 decreases with increasing initial concentration.

The possibility of intra-particle diffusion was explored by using the intra-particle diffusion model [65] (Eq. (3)):

$$k_t = k_i t^{1/2} + I \tag{3}$$

where k_i and I are the intra-particle diffusion rate constant (mg/g min$^{1/2}$) and the intercept, respectively. The plot of q_t vs. $t^{1/2}$ produces the value of k_i as the slope and I as the intercept.

When diffusion makes a difference in adsorption, $q_t - t^{1/2}$ curve will be a straight line. Even, the intercept passes through the origin if intra-particle diffusion is a rate determining step. But, when adsorption involves different mechanisms and speed constants, $q_t - t^{1/2}$ are multi-linearity and for each linear region with the correlation coefficient (r^2) approaching to unity.

The plots of intra-particle diffusion of CR on PLR were given in Fig. 2. Parameters of intra-particle diffusion model were listed in Table 4. Referring to Fig. 2, three distinct linear regions were observed, showing different adsorption mechanisms and speed constants at different interval contact time.

The first part of the curve can be attributed to mass transfer effects taking place with boundary layer diffusion; in this process, the adsorption rate is very high which is resulted from the film diffusion. As time passed by, the rate of adsorption being slowed down, the process of adsorption was controlled by intra-particle diffusion. Finally, the plateau segment indicates the equilibrium state for the adsorption process. The equilibrium stage at the end was due to the decrease in number of active sites available for the adsorption as well as low concentration of CR in the bulk solution.

The intercept did not cross the origin in any of the test conditions, thus suggesting that intra-particle diffusion was not the rate-limiting step.

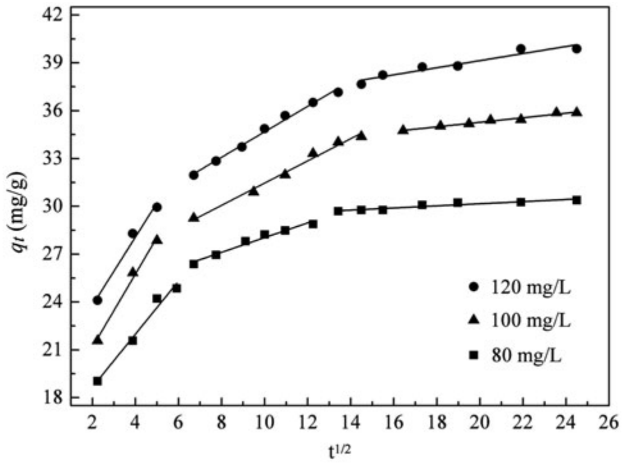

Fig. 2. Intra-particle diffusion plots for CR adsorption onto PLR.

The values of k_i and I for various initial CR concentrations are presented in Table 4. As can be observed, the intra-particle diffusion rate, k_i increases with the increase in initial CR concentration. This results from higher number of CR molecules present in the solution which largely attain the active sites on PLR surface. The values of I also revealed the capaciousness of thickness in boundary layer. As indicated in Table 4, an increase in I values was observed with increase in initial CR concentration. This attributes to greater effect of the boundary layer on higher CR concentration. Thus, thicker the boundary layer surrounding adsorbent eventually higher the uptake of CR.

Table 4
Intra-particle diffusion parameters for the adsorption of CR onto PLR

C_0 (mg/L)	k_i (mg/g min$^{1/2}$)	I	R^2
80	0.4689	23.364	0.982
100	0.6969	24.491	0.980
120	0.7987	26.692	0.992

3.1.3. Adsorption isotherms

Equilibrium studies were performed to evaluate the adsorption capacity of PLR at different temperatures (25, 35, and 45℃) at CR concentration of 100 mg/L. Langmuir [66] and Freundlich [67] equations were applied to describe the adsorption isotherm data by non-linear regression forms:

$$q_e = \frac{q_m b c_e}{1 + b c_e} \tag{4}$$

$$q_e = K_F c_e^{1/n} \tag{5}$$

where C_e (mg/L) is CR equilibrium concentration in the solution, q_e (mg/g) is the adsorption capacity, q_m (mg/g) represents maximum amount of adsorption required to form a homogeneous monolayer at the ACCM, and k_L (L/mg) denotes Langmuir constant to give an account on adsorption energy. The intercept and slope of the linear plot between C_e/q_e vs. C_e give Langmuir constant, k_L and q_m, respectively.

The calculated isotherm constants by non-linear method are listed in Table 5. In terms of the correlation coefficients R^2 values, the experimental data could be well-fitted to the Langmuir isotherm model rather than the Freundlich model, indicating that the adsorption process occurred on the surface of PLR should be monolayer adsorption with homogeneous sites. The maximum adsorption capacities calculated by using the Langmuir model were 45.662, 51.546, and 58.480 mg/g at 25, 35, and 45℃. The value at 25℃ was comparable to the adsorption capacities of some other low-cost adsorbents for CR in Table 6. A comparative evaluation of the adsorbent capacities of various low-cost adsorbents for the adsorption of CR is listed in Table 6. The adsorption capacities of PLR in this study were not among the highest available but a relatively high uptake capacity of CR which makes the PLR suitable for removal of CR in wastewater treatment.

Table 5
Langmuir and Freundlich isotherm parameters for the adsorption of CR onto PLR

Isotherms	Parameters	25℃	35℃	45℃
Langmuir	Q_m (mg/g)	45.662	51.546	58.480
	K_L (L/g)	0.249	0.357	1.089
	R^2	0.9962	0.9976	0.9969
Freundlich	K_F (mg/g)(L/mg)$^{1/n}$	17.296	19.605	29.391
	n	4.671	4.486	5.858
	R^2	0.8729	0.8681	0.8043

Table 6
Reported maximum adsorption capacities (Q_0 in mg/g) in the literature for CR obtained on low-cost adsorbents

Adsorbent	Adsorption capacity Q_0 (mg/g)	Refs.
Deoiled soya	1083.33	[59]
Spent mushroom	147.1	[27]
Coal bottom ash	144.2	[59]
Activated carbons from date pit	105	[24]
Hen feather	73.84	[36]
Ethylenediamine modified wheat straw	68.6	[26]
Pyrolusite leaching residue	45.66	This study
Australian kaolin clay ceram	7.27	[13]
Australian kaolin clay K15GR	6.81	[13]
Australian kaolin clay Q38	5.44	[13]
Activated carbon from coir pith	6.7	[25]
Waste red mud	4.05	[20]

3.1.4. Adsorption thermodynamics

In order to better study the adsorption thermodynamics and effect of temperature on the adsorption, thermodynamic parameters including changes in the Gibbs free energy (ΔG^0, kJ/mol), enthalpy (ΔH^0, kJ/mol), and entropy (ΔS^0, kJ/(mol K)) during the adsorption process are determined by the following equations [68]:

$$G^0 = -RT \ln K_c \tag{6}$$

$$\ln K_c = \frac{\Delta S^0}{R} - \frac{\Delta H^0}{RT} \tag{7}$$

$$K_c = \frac{q_e}{c_e} \tag{8}$$

where K_c is the adsorption scattered coefficients. C_{AE} is the amount of dye (mg) adsorbed on the adsorbent in solution at equilibrium. C_{SE} is the equilibrium concentration (mg L^{-1}) of the dye in the solution. R is gas constant (8.314 J/mol K); T is temperature of solution (K). ΔH^0 and ΔS^0 can be determined from the linear plot of ln K_c vs. $1/T$.

Thermodynamic parameters were listed in Table 7. The free energy changes (ΔG^0) were negative, indicating the spontaneity and feasibility of the process. More negative ΔG^0 values at higher temperature showed that an increase in temperature favored the

Table 7
Thermodynamic parameters of CR onto PLR

Temperature (K)	K_c	ΔG^0 (kJ mol^{-1})	ΔH^0 (kJ mol^{-1})	ΔS^0 (kJ mol^{-1} K^{-1})
298	2.579	−4.51078	83.63	0.287
308	4.886	−6.25018		
318	21.768	−10.4596		

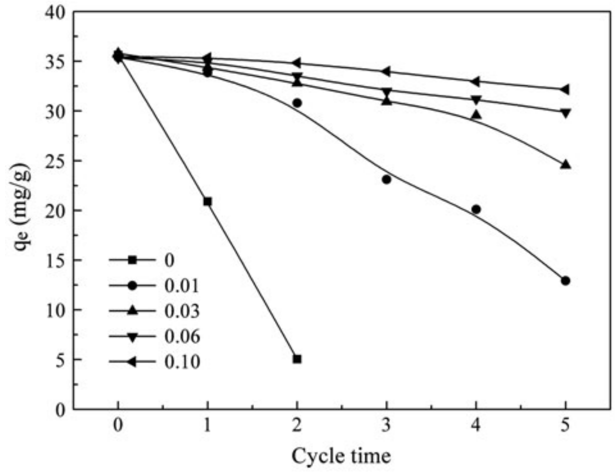

Fig. 3. Variations of adsorption capacities with cycle times under different NaOH concentration in eluent.

adsorption. The positive value of ΔH^0 further confirmed the endothermic nature of the adsorption. Irregular increase of the randomness at the PLR-solution interface during adsorption was also confirmed by the positive value of ΔS^0.

3.2 Desorption and reuse

For the sustainability of adsorption process, studies are carried out to evaluate the reuse potential of PLR. From Fig. 3, two important conclusions could be drawn. First, under all the concentrations, the amount of CR adsorbed decreased with the increasing cycle times. However, the decrease rate decreased with the increasing NaOH concentration in eluent. After five cycles, the removal capacity was decreased from 35.47 to 32.17 when 0.1 mol/L NaOH was used as eluent, indicating that PLR can be reused and readily recycled.

4. Conclusion

The present work showed that PLR was a promising low-cost adsorbent to be used in the removal of CR from aqueous solutions. Adsorption of CR was found to increase with increasing in treatment time and initial concentration. The adsorption system followed pseudo-second-order kinetics. The rate of CR uptake was found to be controlled by both external mass transfer and intra-particle diffusion. The CR uptake process was best described by the Langmuir isotherm with maximum monolayer adsorption capacity of 45.66 mg/g at 25℃. Thermodynamic studies showed CR adsorption onto the PLR was endothermic and spontaneous in nature. The regeneration studies showed that the PLR has good reuse performance. The solution of 0.1 mol/L NaOH was suitable for regeneration. These results revealed that the PLR could be employed as a promising and effective adsorbent for the removal of CR from aqueous solutions.

Acknowledgments

This project is supported by the National Natural Science Foundation of China (NSFC-51374150 and NSFC-51304140), Special Foundation for Young Scientists of Sichuan Province (2011JQ0008), China Postdoctoral Science Foundation funded project (2013M531966) and Postdoctoral Science Foundation funded project of Sichuan Province.

References

[1] G. Crini, Non-conventional low-cost adsorbents for dye removal: A review, Bioresource Technol. 97 (2006) 1061–1085.
[2] P.K. Dutta, An overview of textile pollution and its remedy, Indian J. Environ. Prot. 14 (1994) 443–446.
[3] S. Karcher, A. Kornmuller, M. Jakel, Anion exchange resins for removal of reactive dyes from textile wastewaters, Water Res. 36 (2002) 4717–4724.
[4] M. Wawrzkiewicz, Z. Hubicki, Kinetic studies of dyes sorption from aqueous solutions onto the strongly basic anion-exchanger Lewatit MonoPlus M-600, Chem. Eng. J. 150 (2009) 509–515.
[5] M. Wawrzkiewicz, Z. Hubicki, Equilibrium and kinetic studies on the adsorption of acidic dye by the macroporous anion exchanger, Chem. Eng. J. 157 (2010) 29–34.
[6] M. Greluk, Z. Hubicki, Efficient removal of Acid Orange 7 dye from water using the strongly basic anion exchange resin Amberlite IRA-958, Desalination 278 (2011) 219–226.
[7] P. Gharbani, S.M. Tabatabaii, A. Mehrizad, Removal of Congo red from textile wastewater by ozonation, Int. J. Environ. Sci. Technol. 5 (2008) 495–500.

[8] M. Khadhraoui, H. Trabelsi, M. Ksibi, S. Bouguerra, B. Elleuch, Discoloration and detoxification of a Congo red dye solution by means of ozone treatment for a possible water reuse, J. Hazard. Mater. 161 (2009) 974–981.

[9] R.K. Wahi, W.W. Yu, Y. Liu, M.L. Mejia, J.C. Falkner, W. Nolte, V.L. Colvin, Photo degradation of Congo Red catalyzed by nanosized TiO_2, J. Mol. Catal. A Chem. 242 (2005) 48–56.

[10] M.F. Elahmadi, N. Bensalah, A. Gadri, Treatment of aqueous wastes contaminated with congo red dyes by electrochemical oxidation and ozonation processes, J. Hazard. Mater. 168 (2009) 1163–1169.

[11] K.P. Gopinath, S. Murugesan, J. Abraham, K. Muthukumar, *Bacillus* sp. Mutant for improved biodegradation of Congo red: Random mutagenesis approach, Bioresource Technol. 100 (2009) 6295–6300.

[12] S.D. Kalme, G.K. Parshetti, S.U. Jadhav, S.P. Govindwar, Biodegradation of benzidine based dye Direct Blue-6 by Pseudomonas desmolyticum NCIM 2112, Bioresource Technol. 98 (2007) 1405–1410.

[13] V. Vimonses, S. Lei, B. Jin, Adsorption of congo red by three Australian kaolins, Appl. Clay Sci. 43 (2009) 465–472.

[14] R.A. Shawabkeh, M.F. Tutunji, Experimental study and modeling of basic dye sorption by diatomaceous clay, Appl. Clay Sci. 24 (2003) 111–120.

[15] A.H. Gemeay, A.S. El-Sherbiny, A.B. Zaki, Adsorption and kinetic studies of the intercalation of some organic compounds onto Na^+-montmorillonite, J. Colloid Interf. Sci. 245 (2002) 116–125.

[16] S. Karaca, A. Gürses, Ö. Açışlı, A. Hassani, M. Kıranşan, K. Yıkılmaz, Modeling of adsorption isotherms and kinetics of Remazol Red RB adsorption from aqueous solution by modified clay, Desalin. Water Treat. 51 (2013) 2726–2739.

[17] Z. Al-Qodah, Adsorption of dyes using shale oil ash, Water Res. 34 (2000) 4295–4303.

[18] K.R. Ramakrishna, T. Viraraghavan, Use of slag for dye removal, Waste Manage. 17 (1997) 483–488.

[19] N. Dizge, C. Aydiner, E. Demirbas, M. Kobya, S. Kara, Adsorption of reactive dyes from aqueous solutions by fly ash: Kinetic and equilibrium studies, J. Hazard Mater. 150 (2008) 737–746.

[20] C. Namasivayam, D.J.S.E. Arasi, Removal of congo red from waste water by adsorption onto waste red mud, Chemosphere 34 (1997) 401–417.

[21] V.K. Gupta, A. Mittal, D. Jharec, J. Mittalc, Batch and bulk removal of hazardous colouring agent Rose Bengal by adsorption techniques using bottom ash as adsorbent, RSC Adv. 2 (2012) 8381–8389.

[22] A. Mittal, L. Kurup, Column operations for the removal and recovery of a hazardous dye' Acid Red-27′ from aqueous solutions, using waste materials-bottom ash and de-oiled soya, Ecol. Environ. Conserv. 13(2) (2006) 181–186.

[23] J. Mittal, D. Jhare, H. Vardhan, A. Mittal, Utilization of bottom ash as a low-cost sorbent for the removal and recovery of a toxic halogen containing dye eosin yellow. Desalin. Water Treat., doi: 10.1080/19443994.2013.803265.

[24] M. Belhachemi, F. Addoun, Adsorption of congo red onto activated carbons having different surface properties: Studies of kinetics and adsorption equilibrium, Desalin. Water Treat. 37 (2012) 122–129.

[25] C. Namasivayam, D. Kavitha, Removal of congo red from water by adsorption onto activated carbon prepared from coir pith, an agricultural solid waste, Dyes Pigm. 54 (2002) 47–58.

[26] Z. Wang, P. Han, Y. Jiao, D. Ma, C. Dou, R. Han, Adsorption of congo red using ethylenediamine modified wheat straw, Desalin. Water Treat. 30 (2011) 195–206.

[27] X. Tian, C. Li, H. Yang, Z. Ye, H. Xu, Spent mushroom: A new low-cost adsorbent for removal of Congo Red from aqueous solutions, Desalin. Water Treat. 27 (2011) 319–326.

[28] A. Mittal, V. Thakur, V. Gajbe, Evaluation of adsorption characteristics of an anionic azo dye Brilliant Yellow onto hen feathers in aqueous solutions, Environ. Sci. Pollut. Res. 19 (2012) 2438–2447.

[29] A. Mittal, V. Thakur, V. Gajbe, Adsorptive removal of toxic azo dye Amido Black 10B by hen feather, Environ. Sci. Pollut. Res. 20 (2013) 260–269.

[30] A. Mittal, J. Mittal, L. Kurup, Utilization of hen feathers for the adsorption of Indigo Carmine from simulated effluents, J. Environ. Prot. Sci. 1 (2007) 92–100.

[31] A. Mittal, R. Jain, J. Mittal, S. Varshney, S. Sikarwar, Removal of Yellow ME 7 GL from industrial effluent using electrochemical and adsorption techniques, Int. J. Environ. Pollut. 43(4) (2010) 308–323.

[32] A. Mittal, Removal of the dye, Amaranth from waste water using hen feathers as potential adsorbent, Electron. J. Environ. Agric. Food Chem. 5 (2006) 1296–1305.

[33] A. Mittal, R. Jain, J. Mittal, M. Shrivastava, Adsorptive removal of hazardous dye Quinoline Yellow from wastewater using coconut-husk as potential adsorbent, Fresen. Environ. Bull. 19(6) (2010) 1–9.

[34] A. Mittal, D. Jhare, J. Mittal, Adsorption of hazardous dye Eosin Yellow from aqueous solution onto waste material De-oiled Soya: Isotherm, kinetics and bulk removal, J. Mol. Liq. 179 (2013) 133–140.

[35] H. Daraei, A. Mittal, M. Noorisepehr, F. Daraei, Kinetic and equilibrium studies of adsorptive removal of phenol onto eggshell waste, Environ. Sci. Pollut. Res. 20 (2013) 4603–4611.

[36] A. Mittal, V. Thakur, J. Mittal, H. Vardhan, Process development for the removal of hazardous anionic azo dye Congo red from wastewater by using hen feather as potential adsorbent. Desalin. Water Treat., doi: 10.1080/19443994.2013.785030

[37] J. Mittal, V. Thakur, A. Mittal, Batch removal of hazardous azo dye Bismark Brown R using waste material hen feather, Ecol. Eng. 60 (2013) 249–253.

[38] K.M. Parida, S. Mallick, S.S. Dash, Studies on manganese nodule leached residues: 2. Adsorption of aqueous phosphate on manganese nodule leached residues, J. Colloid Interf. Sci. 290 (2005) 22–27

[39] S. Mallick, S.S. Dash, K.M. Parida, Adsorption of hexavalent chromium on manganese nodule leached residue obtained from NH_3–SO_2 leaching, J. Colloid Interf. Sci. 297 (2006) 419–425.

[40] K.M. Parida, A.C. Pradhan, Removal of phenolic compounds from aqueous solutions by adsorption onto manganese nodule leached residue, J. Hazard Mater. 173 (2010) 758–764.

[41] S.S. Dash, K.M. Parida, Studies on selenite adsorption using manganese nodule leached residues, J. Colloid Interf. Sci. 307 (2007) 333–339.

[42] N.S. Randhawa, N.N. Das, R.K. Jana, Selenite adsorption using leached residues generated by reduction roasting–ammonia leaching of manganese nodules, J. Hazard Mater. 241–242 (2012) 486–492.

[43] K.M. Parida, S. Mallick, B.K. Mohapatra, V.N. Misra, Studies on manganese-nodule leached residues 1. Physicochemical characterization and its adsorption behavior toward Ni^{2+} in aqueous system, J. Hazard Mater. 277 (2004) 48–54.

[44] N.N. Das, R.K. Jana, Adsorption of some bivalent heavy metal ions from aqueous solutions by manganese nodule leached residues, J. Colloid Interf. Sci. 293 (2006) 253–262.

[45] R.N. Sahoo, S.C. Das, B.R. Reddy, P.C. Rath, R.P. Das, Adsorption of copper on manganese nodule residue obtained from NH_3–SO_2 leaching, Hydrometallurgy 62 (2001) 185–192.

[46] A. Agrawal, K.K. Sahu, Kinetic and isotherm studies of cadmium adsorption on manganese nodule residue, J. Hazard Mater. B137 (2006) 915–924.

[47] W. Zhang, C.Y. Cheng, Manganese metallurgy review. Part I: Leaching of ores/secondary materials and recovery of electrolytic/chemical manganese dioxide, Hydrometallurgy 89 (2007) 137–159.

[48] S.C. Das, P.K. Sahoo, P.K. Rao, Extraction of manganese from low-grade manganese ores by ferrous sulfate leaching, Hydrometallurgy 8 (1982) 35–47.

[49] H. Vu, J. Jandova, K. Lisa, F. Vranka, Leaching of manganese deep ocean nodules in $FeSO_4$–SO_4–H_2O solutions, Hydrometallurgy 77 (2005) 147–153.

[50] E.A. Ali, M.A. Shahin, M.S. Ahmed, I.A. Ibrahim, Leaching of low-grade Sinai manganese ore using lactose as a reductant, Egypt J. Chem. 45 (2002) 359–374.

[51] F. Veglio, L. Toro, Fractional factorial-experiments in the development of manganese-dioxide leaching by sucrose in sulfuric-acid-solutions, Hydrometallurgy 36 (1994) 215–230.

[52] C. Acharya, R.N. Kar, L.B. Sukla, Microbial extraction of manganese from low grade manganese ore, Trans. Indian Inst. Met. 54 (2001) 99–103.

[53] C. Abbruzzese, M.Y. Duarte, B. Paponetti, L. Toro, Biological and chemical processing of low-grade manganese ores, Miner. Eng. 3 (1990) 307–318.

[54] J.D. Miller, R. Wan, Reaction kinetics for the leaching of MnO_2 by sulphur dioxide, Hydrometallurgy 10 (1983) 219–242.

[55] P.K. Naik, L.B. Sukla, S.C. Das, Aqueous SO_2 leaching studies on Nishikhal manganese ore through factorial experiment, Hydrometallurgy 54 (2000) 217–228.

[56] G. Senanayake, A mixed surface reaction kinetic model for the reductive leaching of manganese dioxide with acidic sulfur dioxide, Hydrometallurgy 73 (2004) 215–224.

[57] W. Sun, S. Su, Q. Wang, S. Ding, Lab-scale circulation process of electrolytic manganese production with low-grade pyrolusite leaching by SO_2, Hydrometallurgy 133 (2013) 118–125.

[58] C. Abbruzzese, Percolation leaching of manganese ore by aqueous sulfur dioxide, Hydrometallurgy 25 (1990) 85–97.

[59] A. Mittal, J. Mittal, A. Malviya, V.K. Gupta, Adsorptive removal of hazardous anionic dye "Congo red" from wastewater using waste materials and recovery by desorption, J. Colloid Interf. Sci. 340 (2009) 16–26.

[60] <http://en.wikipedia.org/wiki/Congo_red>.

[61] <http://www.sciencelab.com/xMSDS-Congo_red-9927502>.

[62] B.M. Babic, S.K. Milonjic, M.J. Polovina, B.V. Kaludierovic, Point of zero charge and intrinsic equilibrium constants of activated carbon cloth, Carbon 37 (1999) 477–481.

[63] S. Lagergren, Kungliga svenska vetenkapsademiens, Handlingar 24 (1898) 1–39.

[64] Y.S. Ho, G. McKay, Sorption of dye from aqueous solution by peat, Chem. Eng. J. 70 (1998) 115–124.

[65] W.J. Weber Jr, J.C. Morris, Kinetics of adsorption on carbon from solution, J. Sanitary Eng. Div. Am. Soc. Chem. Eng. 89 (1963) 31–59.

[66] I. Langmuir, The adsorption of gases on plane surfaces of glass, mica and platinum, J. Am. Chem. Soc. 40 (1918) 1361–1403.

[67] H. Freundlich, Adsorption in solution, J. Phys. Chem. Soc. 40 (1906) 1361–1368.

[68] H.D. Choi, W.S. Jung, J.M. Cho, B.G. Ryu, J.S. Yang, K. Baek, Adsorption of Cr(VI) onto cationic surfactant-modified activated carbon, J. Hazard. Mater. 166 (2009) 642–646.